Supplementary Information for: "Dense seismic node arrays for enhanced understanding and monitoring of geothermal systems"

T.S. Hudson[1,2], T. Kettley[1], JM. Kendall[1], T. O'Toole[3], A. Jupe[4], R.K. Shail[5], G. Grand[6]

[1] Department of Earth Sciences, University of Oxford, UK
[2] Department of Earth Sciences, ETH Zurich, Switzerland
[3] STRYDE Ltd, UK
[4] Altcom Ltd, UK
[5] Camborne School of Mines, University of Exeter, UK
[6] Eden Geothermal Ltd, UK

Supplementary Information

Parameter	Value
QuakeMigrate detection parameters:	
Data sampling rate	200 Hz
Bandpass filter, P-wave	2-80 Hz
Bandpass filter, S-wave	2-50 Hz
Grid resolution	x = 0.1 km
	y = 0.1 km
	z = 0.2 km
STA/LTA, P-wave	0.05 s / 1.0 s
STA/LTA, S-wave	0.1 s / 1.0 s
Coalescence detection threshold	Median Absolute Deviation (MAD) dynamic trigger with multiplier of 8 and window length of 3600 s.
Moving time window (marginal window)	60 s
Pre/post padding around window	1.0 s
NonLinLoc relocation parameters:	
Arrival-time error	Width of Gaussian fit to QuakeMigrate onset function (STA/LTA) for each receiver
Location method (LOCMETH)	Equal differential time likelihood function (EDT_OT_WT)
Gaussian velocity model error (LOCGAU)	SigmaTime = 0.005 s
Travel-time dependent model error (LOCGAU2)	SigmaTfraction = 0.005 s; SigmaTmin = 0.005 s; SigmaTmax = 10 s

Table S1 – Parameters for earthquake detection using QuakeMigrate and subsequent earthquake relocation using NonLinLoc.

Figure S1 – Example field deployment of 3-component site. Note that this example is for a "stacked" site, where four sensors were deployed in combination for each channel. Typically, most sites only comprise of either one or three nodes (for a Z-only or ZNE sites, respectively). Rubber duck and a person's knees are included for scale.

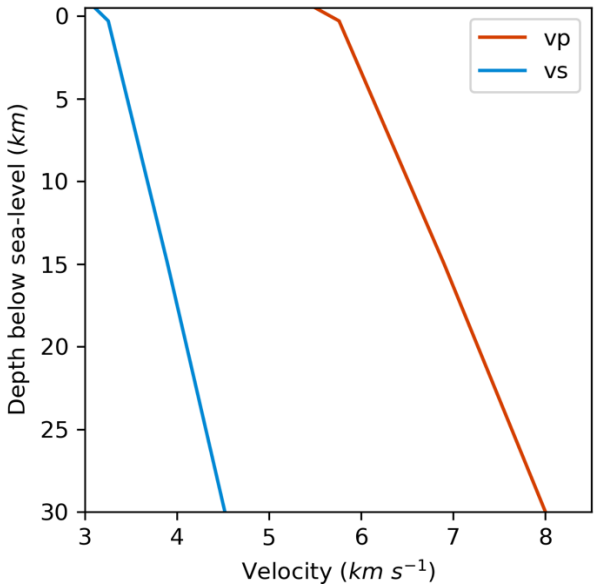

Figure S2 – Velocity model used in this study. This is the British Geological Survey SW England 1D layered model (Booth, 2010).

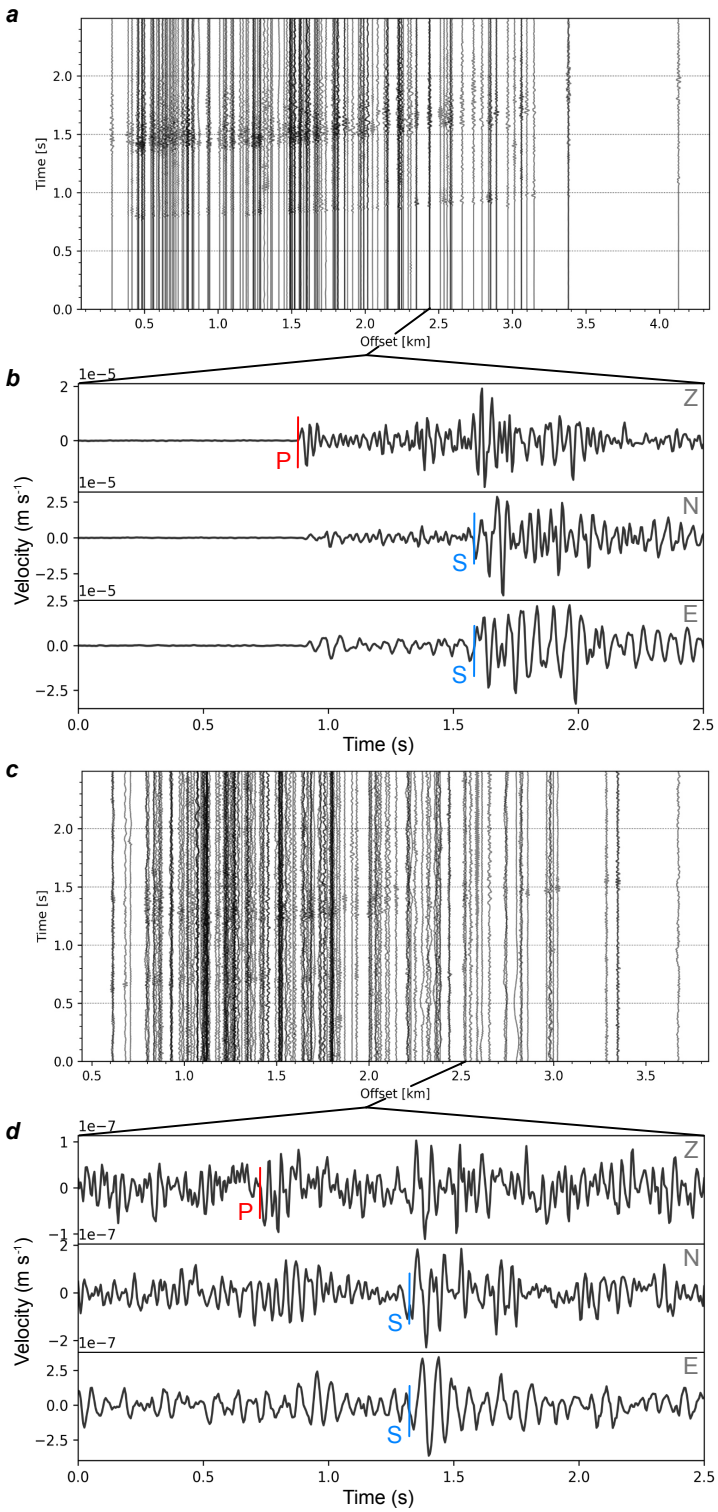

Figure S3 – Example waveforms of a large (M_w = 1.59) and a small (M_w = 1.04) earthquake. a. Record section for an M_w = 1.59 earthquake that occurred at 15:23:04 on 01/12/2022. b. Waveforms for this event at the receiver site F110T (south-west region of the network). c. Record section for an M_w = 1.04 earthquake that occurred at 00:19:38 on 27/11/2022. d. Waveforms for this event at the receiver site F110T (south-west region of the network). P and S arrivals are approximately labelled in (b) and (d). Waveforms have been converted from the native Stryde node units of acceleration to velocity, after correcting for instrument response. Waveforms are then filtered between 1-60 Hz. Note the lower frequency content on the east component, likely due to poorer coupling to the ground, compared to the other channels.

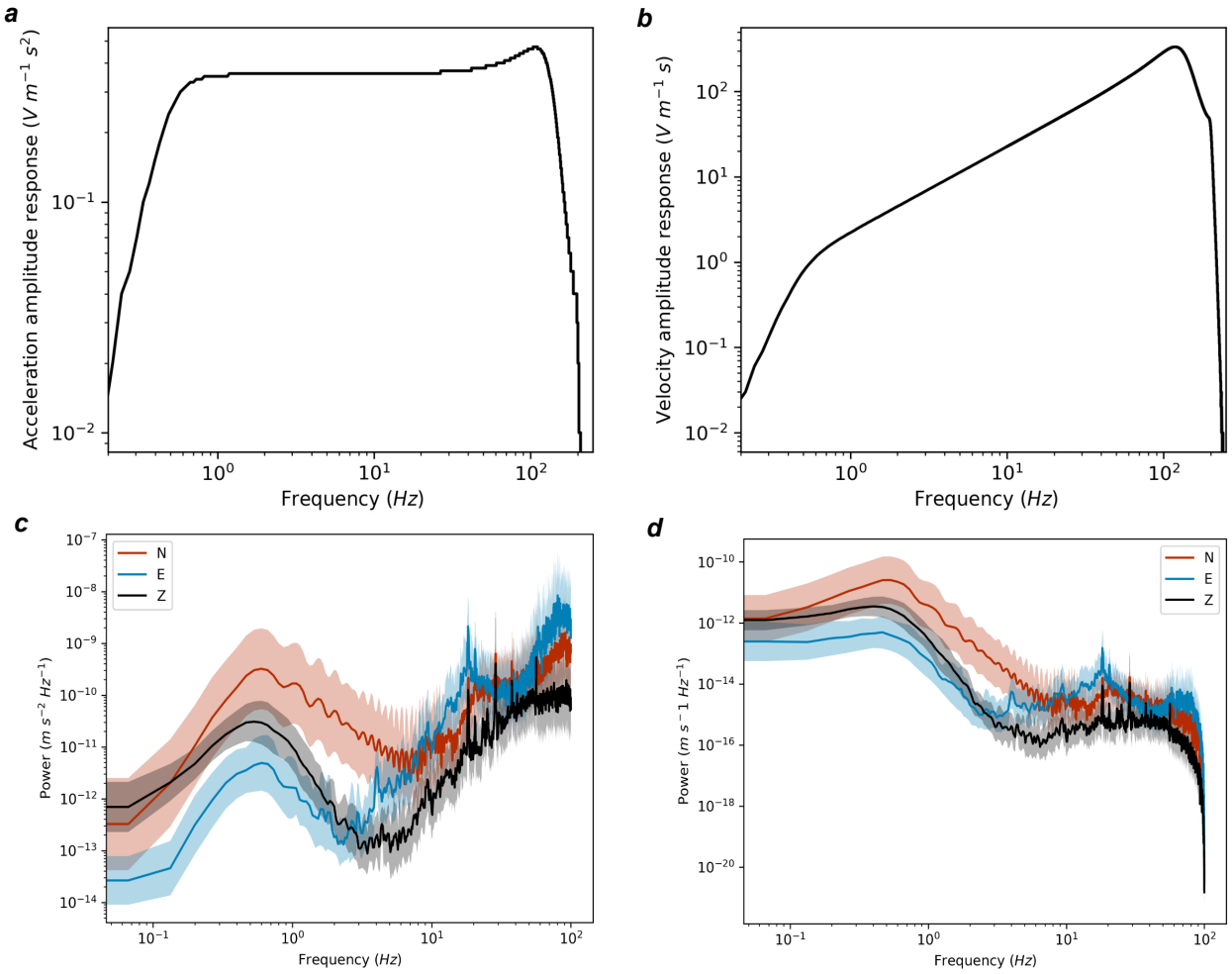

Figure S4 – Stryde node instrument response and example noise spectra. a. Acceleration instrument response. b. Velocity instrument response. Instrument response provided by Stryde Ltd. c. Instrument-response corrected acceleration noise spectra from 50 noise windows at receiver F110T, for all three components. d. Instrument-response corrected velocity noise spectra from 50 noise windows. Variation between noise windows in (c), (d) is shown by shaded region. Spectra in (c), (d) are calculated using a multitaper spectral method.

Parameter	Value
S-wave frequency filter	1-30 Hz
Window start time before fast S-wave arrival time	0.1 s
S-wave arrival time pick tolerance (estimated error)	0.05 s
Window start time after fast S-wave arrival time	0.25 s
Rotation step (increment in ϕ)	1^o
Max. fast to slow S-wave delay-time (δt_{max})	0.25 s
Number of windows for (Teanby et al., 2004)**cluster analysis**	10
Data upsample factor	2

Table S2 – Parameters used for shear-wave splitting analysis (correspond to input parameters used by SWSPy (reference in main text)).

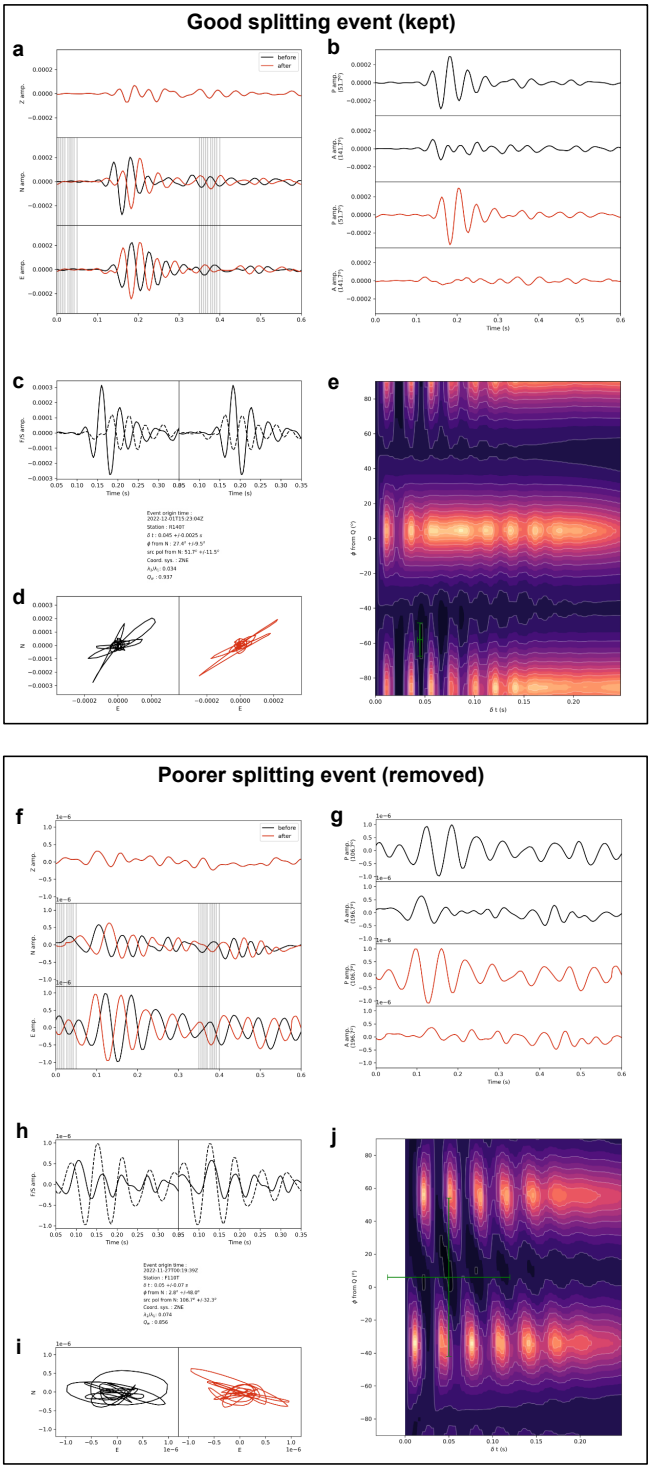

Figure S5 – Examples of good and poor quality splitting measurements. Constraints that make an event deemed good or poor are detailed in the main text. a-e. Examples of a shear-wave good splitting result. a. Waveforms before and after shear-wave splitting effect removed (black and red, respectively). b. Propagation and propagation-perpendicular components, before and after splitting removed. Note that all energy should be in the P-plane. C. Fast and slow shear waves, before and after the time shift is applied. Splitting statistics/parameters are also stated here. D. Particle motions before and after removing splitting effects. e. Fast-direction/time-delay space where the minimum eigenvalue is located (green point). Green bars indicate uncertainty. Note that fast angle is relative to Q-plane, not North. F-j. Same as a-e, but for a

poor splitting event that is removed from the results. See SWSPy (reference in main text) for more details on the underlying analysis and Table S2 for all the parameters used in the shear-wave splitting analysis.

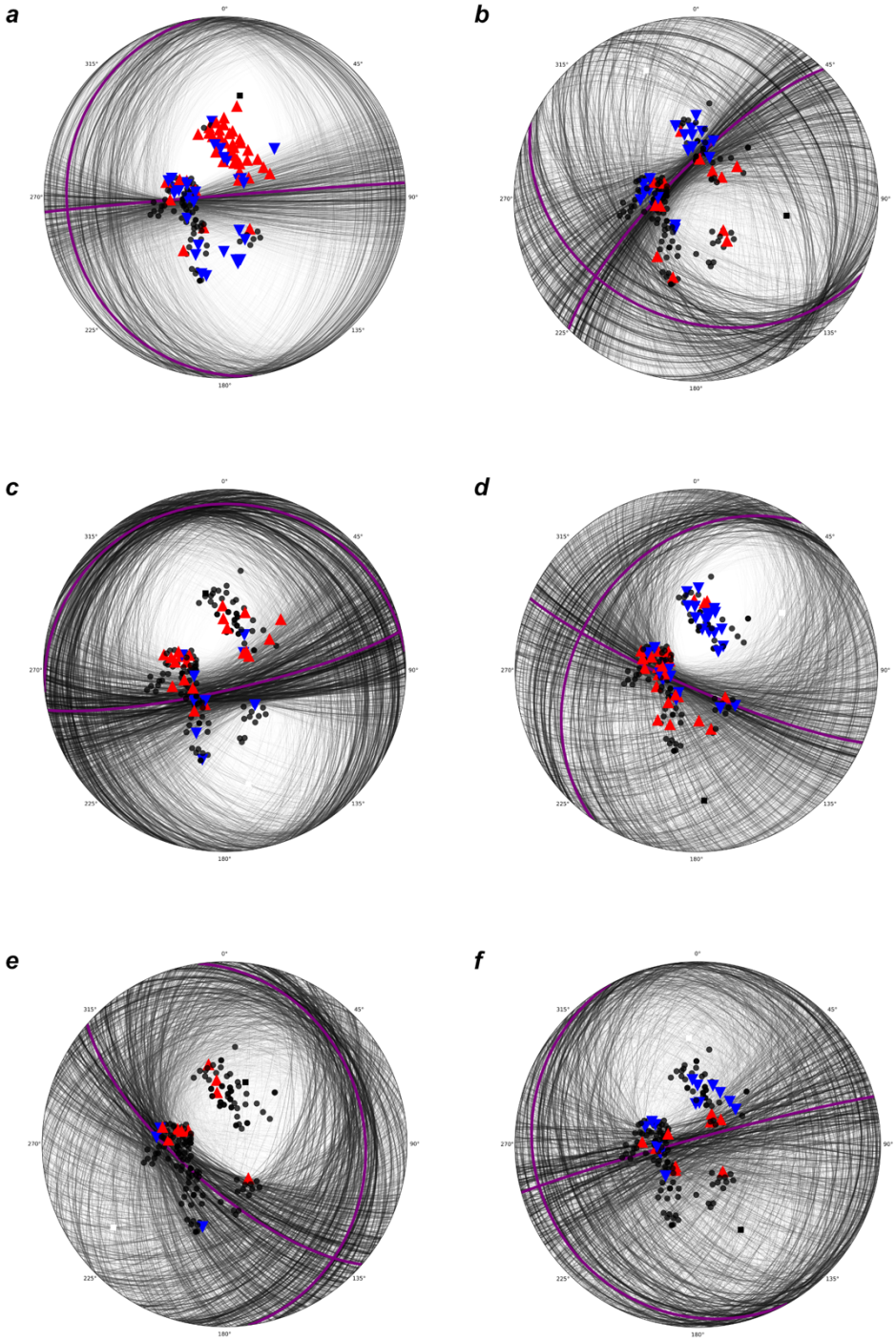

Figure S6 – Examples of other double-couple, automatic P-polarity constrained focal mechanism inversions (corresponding to earthquakes shown in Figure 3a). Red points are receivers with compressional first arrivals, blue points are dilatational first arrivals and black points are undefined. Black lines indicate most likely 1% of fault-plane solutions, which can be thought of as representative of uncertainty in focal mechanism orientation.

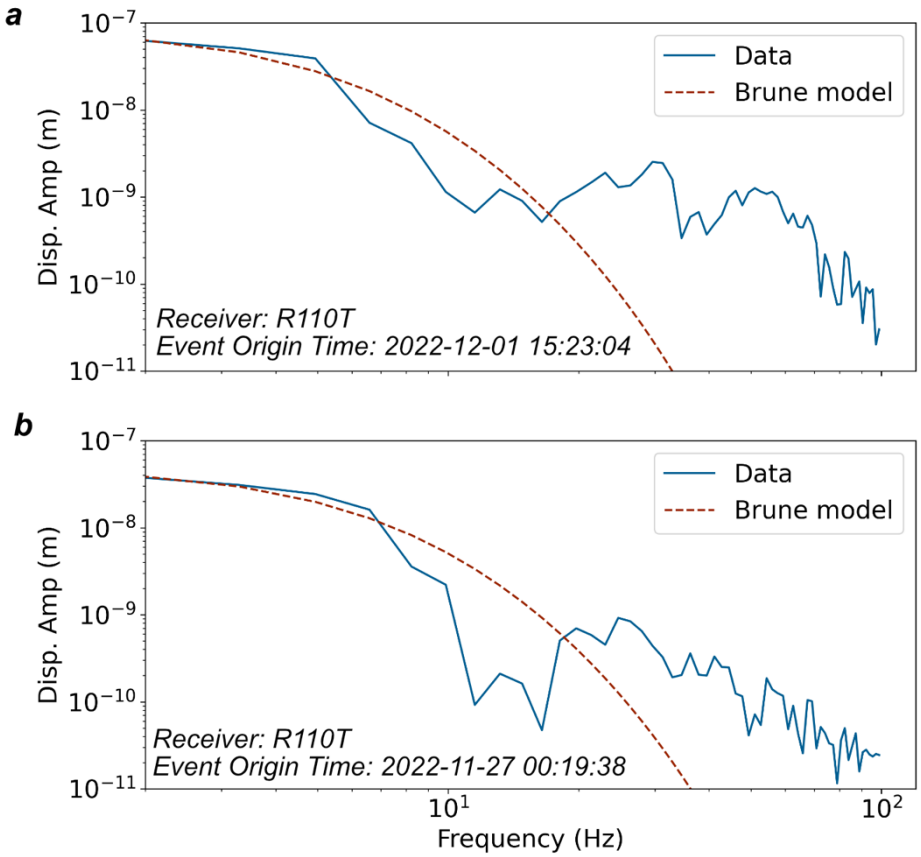

Figure S7 – Examples of earthquake spectra for a larger and smaller magnitude event at one receiver ((a) is the larger event and (b) is the smaller event). Note that higher frequency energy is somewhat not reconciled by Brune model fit, but long-period spectral level, used to calculate moment release, is unaffected.

Supplementary Information References:
(cited here but not in the main text)

Booth, D. C. (2010). UK 1-D regional velocity models by analysis of variance of P-wave travel times from local earthquakes. *Journal of Seismology*, *14*(2), 197–207. https://doi.org/10.1007/s10950-009-9160-4

Teanby, N. A., Kendall, J., & Baan, M. Van Der. (2004). Automation of Shear-Wave Splitting Measurements using Cluster Analysis. *Bulletin of the Seismological Society of America*, *94*(2), 453–463.